

**CAMILA ANGÉLICA SANTOS SOUZA**

**EFFICIENCY OF MAPPING EPISTATIC QUANTITATIVE TRAIT LOCI**

Dissertation submitted to the Genetic and Breeding Graduate Program of the Universidade Federal de Viçosa, as requirement to the title of *Magister Scientiae*.

Adviser: José Marcelo Soriano Viana

**VIÇOSA – MINAS GERAIS  
2022**

Ficha catalográfica elaborada pela Biblioteca Central da Universidade  
Federal de Viçosa - Campus Viçosa

T

S729e Souza, Camila Angélica Santos, 1993-  
2022 Efficiency of mapping epistatic quantitative trait loci /  
Camila Angélica Santos Souza. – Viçosa, MG, 2022.  
1 dissertação eletrônica (26 f.): il.

Texto em inglês.

Inclui apêndice.

Orientador: Jose Marcelo Soriano Viana.

Dissertação (mestrado) - Universidade Federal de Viçosa,  
Departamento de Biologia Geral, 2022.

Referências bibliográficas: f. 20-23.

DOI: <https://doi.org/10.47328/ufvbbt.2022.253>

Modo de acesso: World Wide Web.

1. Mapeamento cromossômico. 2. Epistasia genética.  
3. Reações falso-positivas. 4. Locus de caracteres quantitativos.  
I. Viana, Jose Marcelo Soriano, 1963-. II. Universidade Federal  
de Viçosa. Departamento de Biologia Geral. Programa de  
Pós-Graduação em Genética e Melhoramento. III. Título.

CDD 22. ed.

Bibliotecário(a) responsável: Euzebio Luiz Pinto CRB 6/3317

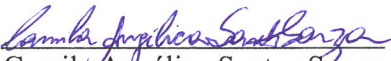
CAMILA ANGÉLICA SANTOS SOUZA


**EFFICIENCY OF MAPPING EPISTATIC QUANTITATIVE TRAIT LOCI**

Dissertation submitted to the Genetic and Breeding Graduate Program of the Universidade Federal de Viçosa, as requirement to the title of *Magister Scientiae*.

APPROVED: March 14, 2022.

Assent:

  
Camila Angélica Santos Souza  
Author

  
José Marcelo Soriano Viana  
Adviser

## **ACKNOWLEDGEMENTS**

To God for gave me strength and patience.

To my parents João Batista and Maria Angélica and my brother Bruno Henrique, that are always by my side giving love and support.

To the Federal University of Viçosa for the opportunity to complete the postgraduate course.

This study was financed in part by the Coordenação de Aperfeiçoamento de Pessoal de Nível Superior – Brasil (CAPES) – Finance Code 001.

To my colleagues that were part of this journey, especially Tatiana Pessoa, Matheus Pereira and Saulo Chaves.

To my adviser and all professor of UFV for share your knowledge.

## ABSTRACT

SOUZA, Camila Angélica Santos, M.Sc., Universidade Federal de Viçosa, March, 2022. **Efficiency of mapping epistatic quantitative trait loci.** Adviser: José Marcelo Soriano Viana.

Previous methodological investigations on epistatic QTL mapping have shown that this procedure is powerful, efficient to control the false positive rate (FPR), and precise to localize QTLs. The objective of this simulation-based study is to show that mapping epistatic QTLs is not almost perfect. The standard procedures for the most important software available maximized the power of detection for QTLs (56-74% on average), associated with a very high FPR (65%) and a low power for the epistatic pairs (7%). Increasing the average power for epistatic pairs (14%) highly increased the related FPR. Adopting a procedure to find the best balance between power and FPR, there was a significant decrease in the power of QTL detection (17-31% on average), associated with a low average power for epistatic pairs (8%) and an average FPR of 31% for QTLs and 16% for epistatic pairs. We believe that the main reasons for these negative results are simplified modelling of the epistatic effects and no inclusion of minor genes (2/3 of the FPR for QTLs were due to minor genes).

**Keywords:** Epistasis. QTL detection power. False positive rate. Mapping precision.

## RESUMO

SOUZA, Camila Angélica Santos, M.Sc., Universidade Federal de Viçosa, março de 2022. **Eficiência do mapeamento de locos epistáticos de característica quantitativa.** Orientador: José Marcelo Soriano Viana.

Investigações metodológicas anteriores sobre mapeamento QTL epistático mostraram que esse procedimento é poderoso, eficiente para controlar a taxa de falso positivo (FP), e preciso para localizar QTLs. O objetivo desse estudo baseado em simulação é mostrar que o mapeamento de QTLs epistáticos não é perfeito. Os procedimentos padrões do *software* mais importante disponível maximizaram o poder de detecção dos QTLs (média de 56-74%), associado a um FP muito alto (65%) e um baixo poder para os pares epistáticos (7%). Aumentar a média do poder para pares epistáticos (14%) aumentou a taxa de FP. Adotando um procedimento para encontrar o melhor equilíbrio entre poder e FP, houve uma diminuição significativa no poder de detecção de QTL (em média 17-31%), associado a uma baixa potência média para pares epistáticos (8%) e um FP médio de 31% para QTLs e 16% para pares epistáticos. Acreditamos que as principais razões para esses resultados negativos sejam a modelagem simplificada dos efeitos epistáticos e a não inclusão de genes menores (2/3 do FP para QTLs foram devidos a genes menores).

**Palavras-chave:** Epistasia. Poder detecção. Falso positivo. Mapeamento QTL.

## LIST OF TABLES

**Table 1** – Power of QTL detection<sup>†</sup>, FPR<sup>†</sup>, and average bias (cM) in the positioning of the true QTLs from the analyses of the first simulation data, using the single- and two-QTL models, the F2 and F2:3 designs, and two sample sizes (200 and 400), assuming no epistasis (No) and an admixture of epistasis types (Ad) and defining thresholds<sup>‡</sup> at 5% from 1,000 (single QTL model) or 100 (two QTLs model) permutations.....24

**Table 2** – Genotypic values of the parents (P1 and P2) and F1 (g/plant), parametric F2 mean and genotypic variance (GV), thresholds<sup>†</sup> at 5% from 100 permutations using data from simulation 1, average power of QTL detection for the low (L), intermediate (I) and high (H) heritability QTLs and for the epistatic QTLs (E), FPR<sup>‡</sup>, and bias (cM) in the positioning of the true QTLs, from the analyses of the F2 data assuming seven epistasis types<sup>§</sup> and an admixture of epistasis types (Ad).....25

## SUMMARY

1. INTRODUCTION.....	8
2. MATERIALS AND METHODS.....	9
2.1 SIMULATION SOFTWARE.....	10
2.2 DATASET.....	11
3. RESULTS.....	13
4. DISCUSSION .....	14
5. APPENDIX .....	17
6. REFERENCES.....	20

## 1. Introduction

Quantitative trait loci (QTL) mapping continues to be an important method for studying the genetic architecture of quantitative traits. Recently, most studies on QTL mapping have used a multiple interval mapping (MIM) model based on a frequentist approach. These investigations have shown that epistasis regularly determines quantitative traits (Goto, Ishikawa, Nishibori, & Tsudzuki, 2019; Xu et al., 2021; Yang et al., 2020), as emphasized by Mackay (2014), although most of the genotypic variance is additive (Hill, Goddard, & Visscher, 2008). In five out of 10 recent published investigations, the epistatic QTL mapping was based on 80 to 200 recombinant inbred lines (RILs), using high single nucleotide polymorphism (SNP) density (one SNP/0.7 to 4.7 cM). The theoretical background for a multiple QTL model with epistasis was developed in a series of studies that included theory and evaluation of the method efficacy, based on field and/or simulated dataset (Boer, Braak, & Jansen, 2002; Carlborg, Andersson, & Kinghorn, 2000; Jannink & Jansen, 2001; C.-H. Kao, Zeng, & Teasdale, 1999; Sen & Churchill, 2001; Yi & Xu, 2002; Yi, Xu, & Allison, 2003).

The MIM model is a multiple QTL model and its likelihood function is a finite normal mixture (C.-H. Kao et al., 1999). From the analysis of field data of a backcross design, C.-H. Kao et al. (1999) observed that MIM identified more QTLs than composite interval mapping and interval mapping. Additionally, the epistasis contributed 10 to 14% of the genotypic variance. Zeng, Kao, and Basten (1999) emphasizes that MIM can improve the power of detection for minor QTL and the precision of estimating QTL positions. For mapping multiple interacting QTLs, Carlborg et al. (2000) proposed a weighted least-squares approach. Based on a simulated  $F_2$  dataset assuming none to 16 QTLs and a single pair of epistatic QTLs, they concluded that the genetic algorithm can be effective for simultaneous mapping of multiple epistatic QTLs. The idea of a two-dimensional scan for searching epistatic QTLs was presented by Sen and Churchill (2001), using a Bayesian framework. From the analysis of field data from a backcross design and based mainly in the two-dimensional scan, the authors declared five QTLs explaining from 3 to 13.5% of the phenotypic variance and two epistatic pairs explaining 6 and 6.5%.

The one-dimensional maximum likelihood approach proposed by Jannink and Jansen (2001) combines across- and within-population information, using three doubled-haploid parents. The authors concluded that the method may double the power to detect first-order epistasis. Boer et al. (2002) proposed a penalized likelihood method for mapping epistatic QTLs

with one-dimensional genome search. The analysis of a simulated backcross dataset including three QTLs and all epistatic digenic interaction effects showed that the inclusion of the epistatic effects increased the QTL power of detection, but under an effective dimension of 3 for epistatic interactions. Other Bayesian frameworks were proposed by Yi et al. (2003) and Yi and Xu (2002). Using three simulated backcross data, Yi et al. (2003) observed no detection of false QTL under a no QTL model, a lower number of detected QTLs when ignoring epistasis, and a high power of detection for the epistatic QTLs. The genetic model adopted by Yi and Xu (2002) includes the additive x additive, additive x dominance, dominance x additive, and dominance x dominance epistatic effects. The analyses of three simulated backcross datasets, assuming two to three QTLs and one, two, and four epistatic effects, showed that fitting the epistatic model improved the power of detection for QTL with no main effect.

Based on the previously described methodological investigations on epistatic QTL mapping, the general conclusion is that this procedure is powerful, efficient to control the false positive rate (FPR), and precise to localize QTLs. That is, the power of detection for individual QTL and for epistatic pairs is close to 100%, there are no false positive QTL or there is an efficient control of the FPR, and the localization of the QTL is very precise. Compared with the almost perfect results from the methodological studies, the investigations of Laurie, Wang, Carlini-Garcia, and Zeng (2014) and Wei, Knott, Haley, and de Koning (2010) provide some more realistic results as the influence of the trait heritability, the epistatic heritability, and the type of epistasis on the detection power of epistatic pairs. However, in both studies there is also an almost perfect control of the FPR and the QTL mapping is very precise. It is surprising a FPR close to zero (0.04) for both individual and epistatic QTLs, associated with a high power of detection, between 78 and 100%. It is also surprising an increase in the power of QTL detection, from 8-16% to 90-99%, associated with a decrease or an insignificant increase in the FPR. We believe that these almost perfect results from simulated datasets are due to a combination of simplification in the definition of the epistatic effects and no inclusion of minor genes. Thus, the objective of this simulation-based study on the efficacy of epistatic QTL mapping is to show that mapping epistatic QTLs is not almost perfect. Differently from the previous studies based on simulation, we included 90 minor genes, defined all digenic epistasis types, and generated the additive, dominance, and the four epistatic genetic values based on Kempthorne (1954).

## **2. Materials and Methods**

## 2.1 Simulation software

The simulated dataset was generated using the software *REALbreeding* (available by request). The program has been developed using Xojo (<https://www.xojo.com/>). *REALbreeding* has been used in studies related to genomic selection (J. M. S. Viana, Pereira, Mundim, Piepho, & Silva, 2018), genome-wide association studies (GWAS) (Pereira, Viana, Andrade, Silva, & Paes, 2018), QTL mapping (J. M. S. Viana, Silva, Mundim, Azevedo, & Jan, 2017), linkage disequilibrium (LD) (Andrade, Viana, Pereira, Pinto, & Fonseca, 2019), population structure (Jose Marcelo Soriano Viana, Valente, Silva, Mundim, & Paes, 2013), heterotic grouping/genetic diversity (José Marcelo Soriano Viana, Risso, Oliveira deLima, & Fonseca e Silva, 2020), and plant breeding (Jose Marcelo Soriano Viana, DeLima, Mundim, Teixeira Conde, & Vilarinho, 2013). It can be also used in human genetics, animal genetics and breeding, population genetics, and evolution. The program simulates individual genotypes for genes and molecular markers and phenotypes in three stages, using inputs from the user. The first stage (genome simulation) is the specification of the number of chromosomes, molecular markers, and genes as well as marker type and density. The second stage (population simulation) is the specification of the population(s) and sample size or progeny number and size. A population is characterized by the average frequency for the genes (biallelic) and markers (first allele). The final stage (trait simulation) is the specification of the minimum and maximum genotypic values for homozygotes, the minimum and maximum phenotypic values (to avoid outliers), the direction and degree of dominance, and the broad sense heritability.

The current version allows the inclusion of digenic epistasis, genotype x environment interaction, and multiple traits, including pleiotropy. The population mean (M) and additive (A), dominance (D), and epistatic (additive x additive (AA), additive x dominance (AD), dominance x additive (DA), and dominance x dominance (DD)) genetic values or general combining ability (GCA), specific combining ability (SCA), and epistatic (I) effects, or genotypic values (G), depending on the population, are calculated from the parametric gene effects and frequencies and the parametric LD values. The population in LD is generated by crossing two populations in linkage equilibrium followed by a generation of random cross. The parametric LD is  $\Delta_{ab}^{(-1)} = [(1 - 2r_{ab})/4](p_{a1} - p_{a2})(p_{b1} - p_{b2})$ , where  $r_{ab}$  is the recombination frequency,  $p$  is an allelic frequency, and the indexes 1 and 2 indicates the parental populations. The phenotypic values ( $P$ ) are computed assuming error effects ( $E$ )

sampled from a normal distribution ( $P = M + A + D + AA + AD + DA + DD + E = G + E$ ,  $P = M + GCA1 + GCA2 + SCA + I + E = G + E$ , or  $P = G + E$ ).

The types of digenic epistasis are: complementary ( $G_{22} = G_{21} = G_{12} = G_{11}$  and  $G_{20} = G_{10} = G_{02} = G_{01} = G_{00}$ ; proportion of 9:7 in a  $F_2$ , assuming independent assortment), duplicate ( $G_{22} = G_{21} = G_{20} = G_{12} = G_{11} = G_{10} = G_{02} = G_{01}$ ; proportion of 15:1 in a  $F_2$ , assuming independent assortment), dominant ( $G_{22} = G_{21} = G_{20} = G_{12} = G_{11} = G_{10}$  and  $G_{02} = G_{01}$ ; proportion of 12:3:1 in a  $F_2$ , assuming independent assortment), recessive ( $G_{22} = G_{21} = G_{12} = G_{11}$ ,  $G_{02} = G_{01}$ , and  $G_{20} = G_{10} = G_{00}$ ; proportion of 9:3:4 in a  $F_2$ , assuming independent assortment), dominant and recessive ( $G_{22} = G_{21} = G_{12} = G_{11} = G_{20} = G_{10} = G_{00}$  and  $G_{02} = G_{01}$ ; proportion of 13:3 in a  $F_2$ , assuming independent assortment), duplicate genes with cumulative effects ( $G_{22} = G_{21} = G_{12} = G_{11}$ , and  $G_{20} = G_{10} = G_{02} = G_{01}$ ; proportion of 9:6:1 in a  $F_2$ , assuming independent assortment), and non-epistatic genic interaction ( $G_{22} = G_{21} = G_{12} = G_{11}$ ,  $G_{20} = G_{10}$ , and  $G_{02} = G_{01}$ ; proportion of 9:3:3:1 in a  $F_2$ , assuming independent assortment).  $G_{ij}$  is the genotypic value for two epistatic genes, where  $i$  and  $j$  ( $i, j = 2, 1, \text{ or } 0$ ) are the numbers of copies of the gene that increases the trait expression. Because the genotypic values for any two interacting genes are not known, there are infinite genotypic values that satisfy the specifications of each type of digenic epistasis. For example, fixing the gene frequencies (the population) and the parameters  $m$ ,  $a$ ,  $d$ , and  $d/a$  (degree of dominance) for each gene (the trait), the solutions  $G_{22} = G_{21} = G_{12} = G_{11} = 5.25$  and  $G_{20} = G_{10} = G_{02} = G_{01} = G_{00} = 5.71$  or  $G_{22} = G_{21} = G_{12} = G_{11} = 6.75$  and  $G_{20} = G_{10} = G_{02} = G_{01} = G_{00} = 2.71$  define complementary epistasis but the genotypic values are not the same. The solution implemented in the software allows the user to control the magnitude of the epistatic variance ( $V(I)$ ), relative to the magnitudes of the additive and dominance variances ( $V(A)$  and  $V(D)$ ). As an input for the user, the software requires the ratio  $V(I)/(V(A) + V(D))$  for each pair of interacting genes (a single value; for example, 1.0). Then, for each pair of interacting genes the software samples a random value for the epistatic value  $I_{22}$  (the epistatic value for the genotype AABB), assuming  $I_{22} \sim N(0, V(I))$ . Finally, the other epistatic effects and genotypic values are computed. In this study, we assumed ratio 1. Increasing the ratio, increases the magnitude of the additive, dominance, and epistatic genetic values.

## 2.2 Dataset

*REALbreeding* crossed two contrasting inbred lines, assuming genes in association, and generated the populations  $F_1$ ,  $F_2$ , and  $F_3$ . The number of simulations of the segregant generations was 50. The sample size for the  $F_2$  and  $F_3$  were 400 and 4000 (400 progeny of size 10). The  $F_2$  plants were genotyped and phenotyped and the  $F_3$  plants were phenotyped. We assumed genotyping for 975 SNPs distributed in 10 chromosomes of 100 cM. The number of SNPs per chromosome ranged from 93 to 100 and the average density was a SNP/cM. We simulated grain yield (g/plant) assuming 10 epistatic QTLs and 90 minor genes (7 to 10 per chromosome). We allocated one QTL in chromosome 1 (Q1), two QTLs in chromosomes 3 (Q2 and Q3), 5 (Q4 and Q5), and 7 (Q6 and Q7), and three QTLs in chromosome 9 (Q8 to Q10). The minimum distance between linked QTLs was 20 cM. The epistatic pairs were Q1-Q5, Q2-Q4, Q3-Q8, Q6-Q7, and Q9-Q10. Thus, we defined two epistatic pairs in the same chromosome and three epistatic pairs in distinct chromosomes. We assumed seven scenarios of same type of epistasis and an admixture of the distinct types. The trait broad sense heritability was 60%. The QTL heritabilities varied from approximately 1 to 13%, depending on the generation and epistasis type (7% on average). In general, one to four QTLs showed heritability between 1 and 5% (low), four to five QTLs had heritability between 6 and 9% (intermediate), and two to three QTLs showed heritability in the range 10 to 13% (high).

#### Efficiency of the epistatic QTL mapping

The dataset was processed using the R package *qtl* (Broman, Wu, Sen, & Churchill, 2003). We used the interval mapping proposed by Lander and Botstein (1989). For computing QTL detection power, FPR, and mapping precision (bias in the QTL positioning), we used a *REALbreeding* tool (eQTL summary). A declared QTL was assumed as a true QTL when the bias between its estimated and actual positions was lower than 20 cM. Because epistatic QTL mapping is more complex for interpreting than non-epistatic QTL mapping, we first processed preliminary analyses using the single- and two-QTL models, the  $F_2$  and  $F_{2:3}$  designs, and two sample sizes (200 and 400), based on the first simulation data assuming no epistasis and an admixture of epistasis types. Because a permutation test based on the expectation-maximization method is extremely time-consuming, we used 1,000 permutations for the single-QTL model but 100 permutations for the two-QTL model. The scenario of no epistasis included six QTLs with heritabilities in the range 6 to 8%. Thus, for both scenarios, the average QTL heritability was 7%. The main questions to be answered were: 1. do the two QTLs model provides a more effective analysis relative to the single QTL model when there is epistasis? 2. does the  $F_{2:3}$

design provide a more effective analysis relative to the  $F_2$  design? and 3. does increasing the sample size significantly improve the epistatic QTL mapping?

### 3. Results

Based on the results from the preliminary analysis (Table 1), we realized that: 1. the two QTLs model provides a more effective analysis relative to the single QTL model when there is epistasis; 2. the  $F_{2:3}$  design did not provide a more effective analysis relative to the  $F_2$  design; and 3. increasing the sample size significantly improves the epistatic QTL mapping. Under no epistasis and higher sample size, note that the power of detection for QTLs with heritability between 6 and 8% was 0.67. The higher FPR (0.20) is attributable to the threshold of 3.9. The FPR would be zero by using a threshold of 4.9 (26% higher). The bias was only 1 cM, on average. Assuming an admixture of epistasis types, note that fitting the two QTLs model to the  $F_2$  or  $F_{2:3}$  data of 400 genotyped plants provided the best results concerning power and FPR. Thus, for assessing the efficacy of the epistatic QTL mapping we used the  $F_2$  data with 400 plants. Under this scenario, the thresholds assuming 100 and 250 permutations were essentially the same. An impressive negative result was a very high FPR under epistasis.

The difference between the parents' genotypic values and the magnitude of the  $F_2$  genotypic variance were lower assuming duplicate epistasis and higher under non-epistatic genic interaction (Table 2). Comparing with the scenario of no epistasis, where the range for the parents and the  $F_2$  genotypic variance were 120 g/plant and  $367.7 \text{ (g/plant)}^2$ , respectively, note that epistasis significantly decreased the difference between parents and the  $F_2$  genotypic variance. This is impressive considering that it was assumed only 10% of epistatic genes. Regardless of the epistasis type, ignoring the maximum LOD for interaction ( $M_i(j, k)$ ) maximizes the power of QTL detection irrespective of the QTL heritability (Table 2). The average power of QTL detection for the low, intermediate, and high heritability QTLs were 56, 67, and 74%, respectively. However, even taking into account the  $M_i(j, k)$  obtained by permutations, the FPR was very high, in the range 60-70%, approximately (65% on average). The high FPR is attributable mainly to the minor genes. The average FPR ignoring the false declarations in chromosomes with no QTL was 45% (range between 40-50%). Thus, we can estimate an average FPR of 23% (range of 15-30%), ignoring minor genes. But minor genes cannot be ignored. Note that taking into account or ignoring  $M_i(j, k)$ , the power of detection for epistatic QTLs is generally zero (average value of only 7%). Only under duplicate and duplicate

genes with cumulative effects, ignoring  $M_i(j, k)$ , we observed one or two epistatic pairs with power greater than or equal to 50%. Interestingly, for these three pairs, only one pair involved high heritability epistatic QTLs. Thus, we did not observe a positive association between power of epistatic QTLs and QTL heritability. As expected, due to the low power of QTL detection, we observed a low FPR for epistatic QTLs (maximum of 15%).

We analyzed the increase in the power of detection for the epistatic QTLs by decreasing the  $M_i(j, k)$  obtained by permutations, but filtering in the file of maximum LODs. But the results were disappointing (Table 2). The average power doubled (14%), but only one to three out of the five epistatic QTLs showed approximate power of at least 10% (this mean that only one in ten similar pairs would be declared) and the FPR was very high (85 to 97%, with one exception). Finally, we investigated the best balance between power of QTL detection and FPR, for both QTLs and epistatic pairs. Again, we filtered in the file of maximum LODs from the analysis ignoring  $M_i(j, k)$ , by specifying a high threshold for the full two-locus model versus a one-locus model. The consequences of keeping a FPR of up to 30% for both QTLs and epistatic pairs were a significant decrease in the power of detection, proportional to the QTL heritability. The average power of detection for the low, intermediate, and low heritability QTLs were 17, 22, and 31, respectively, and the average power of detection for epistatic pairs was 8%.

In regard to the mapping precision, we observed an average bias in the positioning the true declared QTLs in the range 1.1, for duplicate genes with cumulative effects, and 6.0 cM, for duplicate epistasis (Table 2), for the best balance between power of detection and FPR.

#### 4. Discussion

The results from this simulation-based study show that mapping epistatic QTLs is a challenge. Regardless of the epistasis type, the basic procedures of *r/qtl* maximizes the QTL power of detection, by ignoring  $M_i(j, k)$ , but associated with a very high FPR, of approximately 60-70%. Furthermore, it is also disappointing the power to detect the epistatic pairs. Under complementary, recessive, dominant and recessive, and non-epistatic genic interaction, no epistatic pair was detected. For the other epistasis types and admixture of types, only one to two out five epistatic pairs showed a power of at least 10%, approximately, with no clear association between power and the interacting QTL heritabilities (48.7% on average). Broman and Sen (2009) emphasize that they “are inclined to ignore  $M_i(j, k)$ ” in the rule (8.3) and that they “place greater reliance on the numeric summaries from *summary.scantwo*”. But only this procedure

clearly does not provide the best balance between power and FPR for QTLs and epistatic pairs. We emphasize that this negative general result is not due to the use of  $r/ql$ . We also analyzed the first simulation data using Windows QTL Cartographer (Wang, Basten, & Zeng, 2011), performing the sequential search proposed by Laurie et al. (2014), and QTL IciMapping (Meng, Li, Zhang, & Wang, 2015), observing results similar to those provided by  $r/ql$ . The problem is a simplified modelling of epistasis implemented in the software available.

Any software for QTL mapping process the phenotypic and molecular datasets from code specified under quantitative genetics theory. For  $F_2$  data, the genotypic value for two non-epistatic genes is  $G = m_a + m_b + \theta_a a_a + \theta_b a_b + \gamma_a d_a + \gamma_b d_b = M + A + D$ , where, for each gene,  $m$  is the mean of the homozygotes,  $\theta = 1$  and  $\gamma = 0$  if AA or BB,  $\theta = 0$  and  $\gamma = 1$  if Aa or Bb, and  $\theta = -1$  and  $\gamma = 0$  if aa or bb,  $a$  is the deviation between the genotypic value of the homozygote of greater expression and  $m$ ,  $d$  is the dominance deviation (Falconer & Mackay, 1996). The interval mapping is based on the conditional probabilities of the QTL genotypes in an interval flanked by two molecular markers. For example, if there is a QTL in a given interval, the average genotypic value for the individuals with SNP genotype  $mn$  (for the first SNP)  $op$  (for the second SNP) is  $G_{mnop} = M + [P(QQ|mnop) - P(qq|mnop)]a + P(Qq|mnop)d$ , where  $P(QQ|mnop)$ ,  $P(qq|mnop)$ , and  $P(Qq|mnop)$  are the conditional probabilities (Haley & Knott, 1992). Because all software use a correct modelling for the additive and dominance deviations, the QTL mapping of non-epistatic QTLs is really a powerful process that provides an effective control of the FPR and a precise positioning of the true declared QTLs, irrespective of the statistical approach (J. M. S. Viana et al., 2017).

However, correctly modelling epistasis in QTL mapping is a challenge to be overcome. The genotypic value for two interacting genes is  $G = m_a + m_b + \theta_a a_a + \theta_b a_b + \gamma_a d_a + \gamma_b d_b + I = M + A + D + I$ , where  $I$  is the epistatic effect (a specific value for each one of the nine genotypes). Partitioning the epistatic effect based on Kempthorne (1954), we have a much more complex situation:  $G_{ijkl} = M + \alpha_i^1 + \alpha_j^1 + \alpha_k^2 + \alpha_l^2 + \delta_{ij}^1 + \delta_{kl}^2 + (\alpha^1 \alpha^2)_{ik} + (\alpha^1 \alpha^2)_{jk} + (\alpha^1 \alpha^2)_{il} + (\alpha^1 \alpha^2)_{jl} + (\alpha^1 \delta^2)_{ikl} + (\alpha^1 \delta^2)_{jkl} + (\delta^1 \alpha^2)_{ijk} + (\delta^1 \alpha^2)_{ijl} + (\delta^1 \delta^2)_{ijkl} = M + A + D + AA + AD + DA + DD$ , where  $\alpha$  is the average effect of a gene,  $\delta$  is the dominance value, and  $(\alpha\alpha)$ ,  $(\alpha\delta)$ ,  $(\delta\alpha)$ , and  $(\delta\delta)$  are the additive x additive, additive x dominance, dominance x additive, and dominance x dominance effects, respectively. Assuming two epistatic QTLs in two intervals, the 81 parametric average genotypic values in  $F_2$  is complex to derive since the SNP genotype probabilities depend on the gamete probabilities regarding four SNPs and two QTLs. Only in this way the correct coefficients for the epistatic

effects could be derived. In all the previous theoretical studies on epistatic QTL mapping there is a simplified modelling of epistasis. Yi et al. (2003), Boer et al. (2002), Zeng et al. (1999), and C.-H. Kao et al. (1999) assumed that the coefficient of the epistatic effect is the product of the coefficients of the **a** effects, multiplied by an indicator variable, to define if the QTLs are epistatic or not. When modelling individual epistatic effects, the same general rule was assumed (C. H. Kao & Zeng, 2002; Yi & Xu, 2002). That is, the coefficient of the additive x additive effect, for example, was defined as the product between the coefficients for the two **a** deviations (correctly attributed). Even assuming that the SNPs in the first interval have independent assortment (because independence or free recombination (1/2)) relative to the SNPs in the second interval, the coefficients for the epistatic effects do not follow this product rule (see Appendix).

Concerning the differences between this study and the previous investigations on the efficacy of mapping epistatic QTLs, including Laurie et al. (2014) and Wei et al. (2010), our results show that ignoring the effects of minor genes when computing the genotypic values, explain the lower FPR previously observed. This study showed that approximately 2/3 of the FPR was due to minor genes. Furthermore, in the previous studies there is generally a simplified specification of the epistatic effects when generating the simulated genotypic values. Most previous studies on the efficacy of epistatic QTL mapping ignored the types of epistasis and sampled epistatic effects from a Normal distribution, assuming  $I \sim N(0, \sigma_I^2)$ . Only Wei et al. (2010) and Carlborg et al. (2000) considered five to six epistasis types. In regard to high-order epistasis, the epistasis type specification for three or more genes is complex, except for complementary and duplicate (for three epistatic genes, proportions of 27:37 and 63:1, respectively, in a F<sub>2</sub> generation, assuming independent assortment). Based on Kempthorne (1954), the computation of the parametric genetic effects relative to three epistatic genes depends on the F<sub>1</sub> gamete probabilities, where, for example,  $P(ABC) = (1 - r_{ab})(1 - r_{bc})/2$ , assuming no interference. However, Maki-Tanila and Hill (2014) showed that the majority of the epistatic variance is due to two-locus interactions.

The number of applied studies involving epistatic QTL mapping has increased. However, because most of them do not include any information on candidate genes (ontology and level of expression) and gene networks, the investigations do not prove that each declared QTL and epistatic pair are true declarations. Tadmor-Levi, Hulata, and David (2019) and Li et al. (2018) observed QTLs with significant epistatic effects but with one or both interacting QTLs with no significant additive effects. Goto et al. (2019) found 15 pairs of epistatic QTLs from 27 main-

effect QTLs, for chicken body weight. Regarding maize grain yield and five related traits, Yang et al. (2020) found 49 QTLs and 24 epistatic pairs. For rice grain yield and seven related traits, Chen, Tai, Luo, Xiang, and Zhao (2021) found 37 QTLs and 47 epistatic pairs. However, Xu et al. (2021) mapped only two QTLs with significant epistatic effect and Hu et al. (2021) did not find epistatic QTLs using MIM.

Concluding, based on Kempthorne (1954) to simulate the components of the genotypic values assuming 10 epistatic QTLs and 90 minor genes, we show that mapping epistatic QTLs is a challenge. The standard procedures for the most important software available provided high power of detection for QTLs, associated with a low power for the epistatic pairs and a very high FPR for QTLs. Increasing the average power for epistatic QTLs highly increased the related FPR. Adopting a procedure to find the best balance between power and FPR, there was a significantly decrease in the power of QTL detection, associated with a low average power for epistatic pairs and an average FPR of 31% for QTLs and 16% for epistatic pairs. Under the best balance, the procedure is precise for positioning QTLs, showing an average bias of 3.5 cM. We believe that the main reason for these negative results is a simplified modelling of the epistatic effects. However, based on the great flexibility of the software available, we have confidence that breeders can achieve a superior balance between power and FPR when processing field data.

**Acknowledgments** We thank the National Council for Scientific and Technological Development (CNPq), the Brazilian Federal Agency for Support and Evaluation of Graduate Education (Capes; Finance Code 001), and the Foundation for Research Support of Minas Gerais State (Fapemig) for financial support.

**Conflict of Interest** The authors declare no conflict of interest.

**Author Contribution Statement** JMSV designed the study, programmed the software, and revised the manuscript; CASS simulated and processed the data, and wrote the manuscript.

**Data availability:** The dataset is available at <https://doi.org/10.6084/m9.figshare.19242855>.

## 5. Appendix

The coefficients of the epistatic effects in  $F_2$  generation

Assume that there is a QTL in two intervals with independent assortment (due to independence or free recombination;  $Q1/q1$  and  $Q2/q2$ ). Assume also association for the two QTLs and the four flanking SNPs ( $A/a$ ,  $B/b$ ,  $C/c$ , and  $D/d$ ) in the  $F_1$  ( $AQ1BCQ2D/aq1bcq2d$ ).

The gamete probabilities for the  $F_1$  in relation to the first QTL and their flanking markers are well known, given by:

$$P(AQ1B) = P_{111} = P(aq1b) = P_{000} = (1 - r_{aq1})(1 - r_{q1c})/2$$

$$P(Aq1b) = P_{100} = P(aQ1B) = P_{011} = r_{aq1}(1 - r_{q1c})/2$$

$$P(AQ1b) = P_{110} = P(aq1B) = P_{001} = (1 - r_{aq1})r_{q1c}/2$$

$$P(Aq1B) = P_{101} = P(aQ1b) = P_{010} = (1 - I)r_{aq1}r_{q1c}/2$$

where  $I$  is the interference. Assuming  $I = 0$  and defining by  $R$  the gamete probabilities for the  $F_1$  in relation to the second QTL and their flanking markers, we have, for example,

$$P(Q1Q1Q2Q2|AABBCCDD) = \frac{P(AAQ1Q1BB)P(CCQ2Q2DD)}{P(AABB)P(CCDD)} = \frac{P_{111}^2 R_{111}^2}{P_{1.1}^2 R_{1.1}^2}$$

The expectation of the genotypic values for the  $F_2$  individuals with SNP genotype AABBCCDD is

$$E(G|AABBCCDD) = m_1 + m_2 + \alpha_1 a_1 + \alpha_2 a_2 + \delta_1 d_1 + \delta_2 d_2 + I_{2222}$$

where

$$\alpha_1 = \frac{P_{111}^2 - P_{101}^2}{P_{1.1}^2} = \frac{(1 - r_{aq1})^2(1 - r_{q1b})^2 - r_{aq1}^2 r_{q1b}^2}{(1 - r_{aq1} - r_{q1b} + 2r_{aq1}r_{q1b})^2} = \frac{(1 - r_{aq1})^2(1 - r_{q1b})^2 - r_{aq1}^2 r_{q1b}^2}{(1 - r_{ab})^2}$$

$$\delta_1 = \frac{2P_{111}P_{101}}{P_{1.1}^2} = \frac{2r_{aq1}(1 - r_{aq1})r_{q1b}(1 - r_{q1b})}{(1 - r_{ab})^2}$$

$$\alpha_2 = \frac{R_{111}^2 - R_{101}^2}{R_{1.1}^2} = \frac{(1 - r_{cq2})^2(1 - r_{q2d})^2 - r_{cq2}^2 r_{q2d}^2}{(1 - r_{cd})^2}$$

$$\delta_2 = \frac{2R_{111}R_{101}}{R_{1.1}^2} = \frac{2r_{cq2}(1 - r_{cq2})r_{q2d}(1 - r_{q2d})}{(1 - r_{cd})^2}$$

and  $I$  is the average epistatic value for the SNP genotype, given by

$$\begin{aligned}
I_{2222} = & \left( \frac{1}{P_{1.1}R_{1.1}} \right) 4 [P_{111}R_{111}(\alpha_{Q1}\alpha_{Q2}) + P_{111}R_{101}(\alpha_{Q1}\alpha_{q2}) + P_{101}R_{111}(\alpha_{q1}\alpha_{Q2}) \\
& + P_{101}R_{101}(\alpha_{q1}\alpha_{q2})] \\
& + \left( \frac{1}{P_{1.1}R_{1.1}^2} \right) 2 \{ P_{111} [R_{111}^2(\alpha_{Q1}\delta_{Q2Q2}) + 2R_{111}R_{101}(\alpha_{Q1}\delta_{Q2q2}) \\
& + R_{101}^2(\alpha_{Q1}\delta_{q2q2})] \\
& + P_{101} [R_{111}^2(\alpha_{q1}\delta_{Q2Q2}) + 2R_{111}R_{101}(\alpha_{q1}\delta_{Q2q2}) + R_{101}^2(\alpha_{q1}\delta_{q2q2})] \} \\
& + \left( \frac{1}{P_{1.1}^2R_{1.1}} \right) 2 \{ R_{111} [P_{111}^2(\delta_{Q1Q1}\alpha_{Q2}) + 2P_{111}P_{101}(\delta_{Q1q1}\alpha_{Q2}) \\
& + P_{101}^2(\delta_{q1q1}\alpha_{Q2})] \\
& + R_{101} [P_{111}^2(\delta_{Q1Q1}\alpha_{q2}) + 2P_{111}P_{101}(\delta_{Q1q1}\alpha_{q2}) + P_{101}^2(\delta_{q1q1}\alpha_{q2})] \} \\
& + \left( \frac{1}{P_{1.1}^2R_{1.1}^2} \right) [P_{111}^2R_{111}^2(\delta_{Q1Q1}\delta_{Q2Q2}) + P_{111}^22R_{111}R_{101}(\delta_{Q1Q1}\delta_{Q2q2}) \\
& + P_{111}^2R_{101}^2(\delta_{Q1Q1}\delta_{q2q2}) + \dots + P_{101}^2R_{101}^2(\delta_{q1q1}\delta_{q2q2})]
\end{aligned}$$

Note that the coefficients of the a and d deviations are those presented by Haley and Knott (1992). Finally, I think that the expectation-maximization approach will allow the estimation of the epistatic effects under the Kempthorne's restrictions for the epistatic effects (since there is no restrictions for the a and d deviations). Note that there are 81 SNP genotypes and 30 parameters ( $m$ ,  $a_1$ ,  $a_2$ ,  $d_1$ ,  $d_2$ ,  $\alpha_{Q1}\alpha_{Q2}, \dots$ , and  $\delta_{q1q1}\delta_{q2q2}$ ). The Kempthorne's assumptions are (since  $p_1 = p_2 = 1/2$ ):

i) restrictions for the AA effects: 1)  $(\alpha_{Q1}\alpha_{Q2}) + (\alpha_{Q1}\alpha_{q2}) = 0$ ; 2)  $(\alpha_{q1}\alpha_{Q2}) + (\alpha_{q1}\alpha_{q2}) = 0$ ; 3)  $(\alpha_{Q1}\alpha_{Q2}) + (\alpha_{q1}\alpha_{Q2}) = 0$ ; and 4)  $(\alpha_{Q1}\alpha_{q2}) + (\alpha_{q1}\alpha_{q2}) = 0$ .

ii) restrictions for the AD effects: 1)  $(\alpha_{Q1}\delta_{Q2Q2}) + (\alpha_{Q1}\delta_{Q2q2}) = 0$ ; 2)  $(\alpha_{Q1}\delta_{Q2q2}) + (\alpha_{Q1}\delta_{q2q2}) = 0$ ; 3)  $(\alpha_{q1}\delta_{Q2Q2}) + (\alpha_{q1}\delta_{Q2q2}) = 0$ ; 4)  $(\alpha_{q1}\delta_{Q2q2}) + (\alpha_{q1}\delta_{q2q2}) = 0$ ; 5)  $(\alpha_{Q1}\delta_{Q2Q2}) + (\alpha_{q1}\delta_{Q2Q2}) = 0$ ; 6)  $(\alpha_{Q1}\delta_{Q2q2}) + (\alpha_{q1}\delta_{Q2q2}) = 0$ ; and 7)  $(\alpha_{Q1}\delta_{q2q2}) + (\alpha_{q1}\delta_{q2q2}) = 0$  (six out of the seven are independent).

iii) restrictions for the DA effects: 1)  $(\delta_{Q1Q1}\alpha_{Q2}) + (\delta_{Q1q1}\alpha_{Q2}) = 0$ ; 2)  $(\delta_{Q1q1}\alpha_{Q2}) + (\delta_{q1q1}\alpha_{Q2}) = 0$ ; 3)  $(\delta_{Q1Q1}\alpha_{q2}) + (\delta_{Q1q1}\alpha_{q2}) = 0$ ; 4)  $(\delta_{Q1q1}\alpha_{q2}) + (\delta_{q1q1}\alpha_{q2}) = 0$ ; 5)  $(\delta_{Q1Q1}\alpha_{Q2}) + (\delta_{Q1Q1}\alpha_{q2}) = 0$ ; 6)  $(\delta_{Q1q1}\alpha_{Q2}) + (\delta_{Q1q1}\alpha_{q2}) = 0$ ; and 7)  $(\delta_{q1q1}\alpha_{Q2}) + (\delta_{q1q1}\alpha_{q2}) = 0$  (six out of the seven are independent).

iv) restrictions for the DD effects: 1)  $(\delta_{Q_1Q_1}\delta_{Q_2Q_2}) + (\delta_{Q_1Q_1}\delta_{Q_2q_2}) = 0$ ; 2)  $(\delta_{Q_1Q_1}\delta_{Q_2q_2}) + (\delta_{Q_1q_1}\delta_{Q_2q_2}) = 0$ ; 3)  $(\delta_{Q_1q_1}\delta_{Q_2Q_2}) + (\delta_{Q_1q_1}\delta_{Q_2q_2}) = 0$ ; 4)  $(\delta_{Q_1q_1}\delta_{Q_2q_2}) + (\delta_{q_1q_1}\delta_{Q_2Q_2}) = 0$ ; 5)  $(\delta_{q_1q_1}\delta_{Q_2Q_2}) + (\delta_{q_1q_1}\delta_{Q_2q_2}) = 0$ ; 6)  $(\delta_{q_1q_1}\delta_{Q_2q_2}) + (\delta_{q_1q_1}\delta_{q_2q_2}) = 0$ ; 7)  $(\delta_{Q_1Q_1}\delta_{Q_2Q_2}) + (\delta_{Q_1q_1}\delta_{Q_2q_2}) = 0$ ; 8)  $(\delta_{Q_1q_1}\delta_{Q_2Q_2}) + (\delta_{q_1q_1}\delta_{Q_2Q_2}) = 0$ ; 9)  $(\delta_{Q_1Q_1}\delta_{Q_2q_2}) + (\delta_{Q_1q_1}\delta_{Q_2q_2}) = 0$ ; 10)  $(\delta_{Q_1q_1}\delta_{Q_2q_2}) + (\delta_{q_1q_1}\delta_{Q_2q_2}) = 0$ ; 11)  $(\delta_{Q_1Q_1}\delta_{q_2q_2}) + (\delta_{Q_1q_1}\delta_{q_2q_2}) = 0$ ; and 12)  $(\delta_{Q_1q_1}\delta_{q_2q_2}) + (\delta_{q_1q_1}\delta_{q_2q_2}) = 0$  (nine out of the 12 are independent).

## 6. References

- Andrade, A. C. B., Viana, J. M. S., Pereira, H. D., Pinto, V. B., & Fonseca, E. S. F. (2019). Linkage disequilibrium and haplotype block patterns in popcorn populations. *PLoS One*, *14*(9), e0219417. doi:10.1371/journal.pone.0219417
- Boer, M. P., Braak, C. J. F., & Jansen, R. C. (2002). A Penalized Likelihood Method for Mapping Epistatic Quantitative Trait Loci With One-Dimensional Genome Searches. *Genetics*, *162*, 951–960.
- Broman, K. W., & Sen, S. (2009). *A Guide to QTL Mapping with R/qtl*: Springer.
- Broman, K. W., Wu, H., Sen, S., & Churchill, G. A. (2003). R/qtl: QTL mapping in experimental crosses. *Bioinformatics*, *19*(7), 889–890. doi:10.1093/bioinformatics/btg112
- Carlborg, O., Andersson, L., & Kinghorn, B. (2000). The Use of a Genetic Algorithm for Simultaneous Mapping of Multiple Interacting Quantitative Trait Loci. *Genetics*, *155*, 2003–2010.
- Chen, J., Tai, L. Y., Luo, L., Xiang, J., & Zhao, Z. W. (2021). Mapping QTLs for yield component traits using overwintering cultivated rice. *Journal of Genetics*, *100*(2). doi:10.1007/s12041-021-01279-1
- Falconer, D. S., & Mackay, T. F. C. (1996). *Introduction to Quantitative Genetics*.
- Goto, T., Ishikawa, A., Nishibori, M., & Tsudzuki, M. (2019). A longitudinal quantitative trait locus mapping of chicken growth traits. *Molecular Genetics and Genomics*, *294*(1), 243–252. doi:10.1007/s00438-018-1501-y
- Haley, C. S., & Knott, S. A. (1992). A simple regression method for mapping quantitative trait loci in line crosses using flanking markers. *Heredity (Edinb)*, *69*, 15–324.
- Hill, W. G., Goddard, M. E., & Visscher, P. M. (2008). Data and theory point to mainly additive genetic variance for complex traits. *Plos Genetics*, *4*(2). doi:10.1371/journal.pgen.1000008

- Hu, S. T., Wang, M., Zhang, X., Chen, W. K., Song, X. R., Fu, X. Y., . . . Yang, X. H. (2021). Genetic basis of kernel starch content decoded in a maize multi-parent population. *Plant Biotechnology Journal*, *19*(11), 2192-2205. doi:10.1111/pbi.13645
- Jannink, J.-L., & Jansen, R. (2001). Mapping Epistatic Quantitative Trait Loci With One-Dimensional Genome Searches. *Genetics*, *157*, 445-454.
- Kao, C.-H., Zeng, Z.-B., & Teasdale, R. D. (1999). Multiple Interval Mapping for Quantitative Trait Loci. *Genetics*, *152*, 1203-1216.
- Kao, C. H., & Zeng, Z. B. (2002). Modeling epistasis of quantitative trait loci using Cockerham's model. *Genetics*, *160*(3), 1243-1261.
- Kempthorne, O. (1954). The theoretical values of correlations between relatives in random mating populations. *Genetics*, *40*, 153-167.
- Lander, E. S., & Botstein, D. (1989). Mapping Mendelian Factors Underlying Quantitative Traits Using RFLP Linkage Maps. *Genetics*, *121*, 185-199.
- Laurie, C., Wang, S., Carlini-Garcia, L. A., & Zeng, Z. B. (2014). Mapping epistatic quantitative trait loci. *BMC Genet*, *15*, 112.
- Li, J. C., Huang, W., Cao, H. J., Xiao, G. L., Zhou, J., Xie, C. H., . . . Song, B. T. (2018). Additive and epistatic QTLs underlying the dormancy in a diploid potato population across seven environments. *Scientia Horticulturae*, *240*, 578-584. doi:10.1016/j.scienta.2018.06.071
- Mackay, T. F. C. (2014). Epistasis and quantitative traits: using model organisms to study gene-gene interactions. *Nature Reviews Genetics*, *15*(1), 22-33. doi:10.1038/nrg3627
- Maki-Tanila, A., & Hill, W. G. (2014). Influence of Gene Interaction on Complex Trait Variation with Multilocus Models. *Genetics*, *198*(1), 355-367. doi:10.1534/genetics.114.165282
- Meng, L., Li, H., Zhang, L., & Wang, J. (2015). QTL IciMapping: Integrated software for genetic linkage map construction and quantitative trait locus mapping in biparental populations. *The Crop Journal*, *3*(3), 269-283. doi:10.1016/j.cj.2015.01.001
- Pereira, H. D., Viana, J. M. S., Andrade, A. C. B., Silva, F. F. E., & Paes, G. P. (2018). Relevance of genetic relationship in GWAS and genomic prediction. *Journal of Applied Genetics*, *59*(1), 1-8. doi:10.1007/s13353-017-0417-2
- Sen, S., & Churchill, G. A. (2001). A Statistical Framework for Quantitative Trait Mapping. *Genetics*, *159*, 371-387.

- Tadmor-Levi, R., Hulata, G., & David, L. (2019). Multiple interacting QTLs affect disease challenge survival in common carp (*Cyprinus carpio*). *Heredity (Edinb)*, *123*(5), 565-578. doi:10.1038/s41437-019-0224-0
- Viana, J. M. S., DeLima, R. O., Mundim, G. B., Teixeira Conde, A. B., & Vilarinho, A. A. (2013). Relative efficiency of the genotypic value and combining ability effects on reciprocal recurrent selection. *Theoretical and Applied Genetics*, *126*(4), 889-899. doi:10.1007/s00122-012-2023-3
- Viana, J. M. S., Pereira, H. D., Mundim, G. B., Piepho, H. P., & Silva, F. F. E. (2018). Efficiency of genomic prediction of non-assessed single crosses. *Heredity (Edinb)*, *120*(4), 283-295. doi:10.1038/s41437-017-0027-0
- Viana, J. M. S., Risso, L. A., Oliveira deLima, R., & Fonseca e Silva, F. (2020). Factors affecting heterotic grouping with cross-pollinating crops. *Agronomy Journal*. doi:10.1002/agj2.20485
- Viana, J. M. S., Silva, F. F., Mundim, G. B., Azevedo, C. F., & Jan, H. U. (2017). Efficiency of low heritability QTL mapping under high SNP density. *Euphytica*, *213*(1). doi:10.1007/s10681-016-1800-5
- Viana, J. M. S., Valente, M. S. F., Silva, F. F., Mundim, G. B., & Paes, G. P. (2013). Efficacy of population structure analysis with breeding populations and inbred lines. *Genetica*, *141*(7-9), 389-399. doi:10.1007/s10709-013-9738-1
- Wang, S., Basten, C. J., & Zeng, Z. B. (2011). WINDOWS QTL Cartographer.
- Wei, W. H., Knott, S., Haley, C. S., & de Koning, D. J. (2010). Controlling false positives in the mapping of epistatic QTL. *Heredity (Edinb)*, *104*(4), 401-409. doi:10.1038/hdy.2009.129
- Xu, Y. F., La, G. X., Fatima, N., Liu, Z. H., Zhang, L. R., Zhao, L. F., . . . Bai, G. H. (2021). Precise mapping of QTL for Hessian fly resistance in the hard winter wheat cultivar 'Overland'. *Theoretical and Applied Genetics*, *134*(12), 3951-3962. doi:10.1007/s00122-021-03940-w
- Yang, J. W., Liu, Z. H., Chen, Q., Qu, Y. Z., Tang, J. H., Lubberstedt, T., & Li, H. C. (2020). Mapping of QTL for Grain Yield Components Based on a DH Population in Maize. *Scientific Reports*, *10*(1). doi:10.1038/s41598-020-63960-2
- Yi, N., & Xu, S. (2002). Mapping quantitative trait loci with epistatic effects. *Genet Res (Camb)*, *79*(02). doi:10.1017/s0016672301005511

- Yi, N., Xu, S., & Allison, D. B. (2003). Bayesian Model Choice and Search Strategies for Mapping Interacting Quantitative Trait Loci. *Genetics*, *165*, 867–883.
- Zeng, Z. B., Kao, C. H., & Basten, C. J. (1999). Estimating the genetic architecture of quantitative traits. *Genetical Research*, *74*(3), 279-289. doi:10.1017/s0016672399004255

**Table 1** Power of QTL detection<sup>†</sup>, FPR<sup>†</sup>, and average bias (cM) in the positioning of the true QTLs from the analyses of the first simulation data, using the single- and two-QTL models, the F<sub>2</sub> and F<sub>2:3</sub> designs, and two sample sizes (200 and 400), assuming no epistasis (No) and an admixture of epistasis types (Ad) and defining thresholds<sup>‡</sup> at 5% from 1,000 (single QTL model) or 100 (two QTLs model) permutations

Genetic model	Statistical model	Design	Sample	Threshold(s)	Power	FPR	Bias	
No	Single QTL	F <sub>2</sub>	200	3.77	0.50	0.25	2.4	
			400	3.88	0.67	0.20	1.3	
		F <sub>2:3</sub>	200	3.69	0.83	0.00	2.5	
			400	3.87	0.67	0.20	0.6	
Ad	Single QTL	F <sub>2</sub>	200	3.69	0.10	0.67	4.4	
			400	3.68	0.40	0.56	8.0	
		F <sub>2:3</sub>	200	3.89	0.10	0.80	20.2	
			400	3.76	0.10	0.87	20.2	
		Two QTLs	F <sub>2</sub>	200	8.9; 7.1; 6.0; 6.2; 3.6	0.50/0.00	0.61/0.00	5.6
				400	9.2; 7.1; 5.9; 6.7; 4.0	0.60/0.00	0.67/0.00	8.3
	F <sub>2:3</sub>		200	9.1; 7.0; 5.8; 6.3; 3.9 <sup>§</sup>	0.60/0.00	0.67/0.00	8.3	
			400	9.6; 7.4; 6.5; 6.7; 3.7	0.40/0.00	0.75/0.00	7.1	
			400	9.3; 7.0; 5.9; 6.4; 4.1	0.60/0.00	0.67/0.00	7.2	

<sup>†</sup>The values after / refer to the power of detection/FPR for epistatic QTLs.

<sup>‡</sup>The five LOD thresholds are for testing the full two-locus model versus the null (no QTL) model, the two locus additive model versus the null model, interaction, the full two-locus model versus a one-locus model, and the two locus additive model versus a one-locus model.

<sup>§</sup>250 permutations.

**Table 2** Genotypic values of the parents (P<sub>1</sub> and P<sub>2</sub>) and F<sub>1</sub> (g/plant), parametric F<sub>2</sub> mean and genotypic variance (GV), thresholds<sup>†</sup> at 5% from 100 permutations using data from simulation 1, average power of QTL detection for the low (L), intermediate (I) and high (H) heritability QTLs and for the epistatic QTLs (E), FPR<sup>‡</sup>, and bias (cM) in the positioning of the true QTLs, from the analyses of the F<sub>2</sub> data assuming seven epistasis types<sup>§</sup> and an admixture of epistasis types (Ad)

Epistasis	P <sub>1</sub>	P <sub>2</sub>	F <sub>1</sub>	F <sub>2</sub>	GV	Thresholds	Power			E <sup>¶</sup>	FPR	Bias
							L	I	H			
Co	148.5	85.3	136.7	126.5	63.1	9.0; 7.0; 6.1; 6.4; 3.9	0.30	0.47	0.16	0.00/0.00/0.00/0.00/0.00	0.65/0.02	5.4
						9.0; 7.0; 0.0; 6.4; 3.9	0.50	0.72	0.75	0.00/0.00/0.00/0.00/0.00	0.66/0.02	6.3
						9.0; 7.0; 2.0; 6.4; 3.9	0.50	0.72	0.75	0.24/0.00/0.00/0.00/0.06	0.66/0.96	6.3
						24.5; 7.0; 2.0; 6.4; 3.9	0.19	0.28	0.06	0.20/0.00/0.00/0.00/0.00	0.30/0.32	3.8
Du	128.4	98.6	116.6	110.6	52.2	9.4; 7.3; 6.0; 6.3; 4.5	0.13	0.40	0.40	0.00/0.00/0.00/0.92/0.00	0.62/0.10	5.9
						9.4; 7.3; 0.0; 6.3; 4.5	0.39	0.51	0.72	0.00/0.00/0.00/0.92/0.00	0.70/0.10	7.2
						18.5; 7.3; 6.0; 6.3; 4.5	0.03	0.14	0.07	0.00/0.00/0.00/0.16/0.00	0.32/0.05	6.0
Do	137.8	67.0	126.0	119.3	62.4	8.4; 5.8; 4.7; 5.7; 3.0	0.86	0.51	0.53	0.18/0.24/0.00/0.00/0.00	0.61/0.15	6.5
						8.4; 5.8; 0.0; 5.7; 3.0	0.93	0.63	0.73	0.18/0.24/0.00/0.00/0.00	0.65/0.15	6.6
						8.4; 5.8; 2.0; 5.7; 3.0	0.93	0.63	0.73	0.34/0.54/0.00/0.02/0.20	0.65/0.89	6.6
						16.5; 5.8; 3.0; 5.7; 3.0	0.36	0.28	0.19	0.18/0.18/0.00/0.00/0.00	0.30/0.16	4.5
Re	145.4	91.4	133.6	125.8	68.4	9.3; 7.0; 5.8; 6.6; 4.2	0.60	0.37	0.08	0.00/0.00/0.00/0.00/0.00	0.56/0.00	3.4
						9.3; 7.0; 0.0; 6.6; 4.2	0.73	0.58	0.54	0.00/0.00/0.00/0.00/0.00	0.67/0.00	5.1
						9.3; 7.0; 2.0; 6.6; 4.2	0.73	0.58	0.54	0.72/0.04/0.00/0.00/0.00	0.67/0.91	5.1
						20.0; 7.0; 2.5; 6.6; 4.2	0.48	0.29	0.06	0.42/0.00/0.00/0.00/0.00	0.32/0.34	2.7
DR	143.8	82.8	132.0	122.1	61.3	9.1; 6.8; 5.6; 6.6; 4.4	0.29	0.21	0.34	0.00/0.00/0.00/0.00/0.02	0.69/0.02	5.3
						9.1; 6.8; 0.0; 6.6; 4.4	0.63	0.59	0.68	0.00/0.00/0.00/0.00/0.02	0.67/0.02	6.9
						9.1; 6.8; 2.0; 6.6; 4.4	0.63	0.59	0.68	0.10/0.00/0.00/0.18/0.16	0.67/0.95	6.9
						26.0; 6.8; 5.6; 6.6; 4.4	0.16	0.11	0.06	0.00/0.00/0.00/0.00/0.00	0.32/0.00	2.5
Dg	140.0	88.4	128.2	126.6	63.3	7.7; 6.1; 5.3; 4.9; 2.9	0.28	0.53	1.00	0.50/0.00/0.00/0.00/1.00	0.64/0.01	4.0

						7.7; 6.1; 0.0; 4.9; 2.9	0.45	0.86	1.00	0.50/0.00/0.00/0.00/1.00	0.67/0.01	5.4
						7.7; 6.1; 2.0; 4.9; 2.9	0.45	0.86	1.00	0.76/0.00/0.00/0.18/1.00	0.67/0.85	5.4
						13.5; 6.1; 5.3; 4.9; 2.9	0.04	0.08	1.00	0.14/0.00/0.00/0.00/1.00	0.29/0.01	1.1
Ne	148.8	71.0	137.1	123.3	69.8	10.3; 6.8; 5.0; 7.8; 4.0	0.35	0.58	0.34	0.02/0.00/0.00/0.00/0.00	0.62/0.06	6.3
						10.3; 6.8; 0.0; 7.8; 4.0	0.51	0.80	0.51	0.02/0.00/0.00/0.00/0.00	0.65/0.06	6.9
						10.3; 6.8; 2.0; 7.8; 4.0	0.51	0.80	0.51	0.16/0.02/0.00/0.10/0.00	0.65/0.97	6.9
						21.5; 6.8; 3.0; 7.8; 4.0	0.18	0.40	0.07	0.12/0.00/0.00/0.00/0.00	0.30/0.20	4.5
Ad	146.9	78.7	135.1	122.6	56.9	9.2; 6.9; 5.5; 6.6; 3.8	0.05	0.41	0.91	0.00/0.00/0.00/0.00/0.08	0.68/0.04	6.1
						9.2; 6.9; 0.0; 6.6; 3.8	0.38	0.69	0.99	0.00/0.00/0.00/0.00/0.08	0.67/0.04	7.3
						9.2; 6.9; 2.0; 6.6; 3.8	0.38	0.69	0.99	0.00/0.02/0.02/0.00/0.72	0.67/0.91	7.3
						24.0; 6.9; 2.0; 6.6; 3.8	0.02	0.08	0.63	0.00/0.00/0.00/0.00/0.40	0.32/0.18	3.0

†The five LOD thresholds are for testing the full two-locus model versus the null (no QTL) model, the two locus additive model versus the null model, interaction, the full two-locus model versus a one-locus model, and the two locus additive model versus a one-locus model (Broman & Sen, 2009); the 2nd row thresholds ignore the LOD for interaction in the rule in equation (8.3) of Broman and Sen (2009); the 3<sup>rd</sup> row thresholds maximizes the power for epistatic QTLs; the 4<sup>th</sup> row thresholds provides the best balance between power and FDR.

‡The values after / refer to the FPR for epistatic QTLs.

§Co = complementary, Du = duplicate, Do = dominant, Re = recessive, DR = dominant and recessive, Dg = duplicate genes with cumulative effects, and Ne = non-epistatic genic interaction.

¶LxI, LxL, LxI, IxI, and HxH for Co, Dg, and Ne, IxI, LxI, LxI, IxH, and HxH for Du, LxI, LxL, IxI, IxI, and HxH for Do, Re, and DR, and LxI, LxI, IxI, and HxH for Ad.